Soliton-induced supercontinuum generation in liquid-filled photonic crystal fibre

K PORSEZIAN[1,*] and R VASANTHA JAYAKANTHA RAJA[2]

[1]Department of Physics, School of Physical, Chemical and Applied Sciences,
Pondicherry University, Puducherry 605 014, India
[2]Central University of Tamil Nadu, Thiruvarur 610 001, India
*Corresponding author. E-mail: ponzsol@yahoo.com

Abstract. We aim to study the nonlinear optical phenomena with ultra-broadband radiation in photonic crystal fibre (PCF). While PCFs with cores made from different glasses are well studied in previous works, in this paper, it is planned to investigate the dynamics of nonlinear processes of supercontinuum generation (SCG) in liquid-filled PCF (LCPCF) to understand the physical phenomena of femtosecond pulse propagation, particularly, the temporal and spectral changes of the pulse propagating through specific PCFs. Since the CS_2-filled LCPCF has complex nonlinear phenomena, we intend to analyse the role of saturable nonlinear response and slow nonlinear response on SCG in detail. For the physical explanation, soliton fission and modulational instability techniques will be implemented to investigate the impact of slow nonlinear response and saturable nonlinear response respectively, in SCG process.

Keywords. Photonic crystal fibre; supercontinuum generation; reorientational nonlinearity; saturable nonlinearity.

PACS Nos 42.81.Qb; 42.65.Wi; 42.70.Jk; 42.65.Jx; 42.65.Pc; 82.35.Np

1. Introduction

In recent years, intensive and different aspects of investigations of photonic crystal fibres (PCFs) have received great deal of scientific attention because of their numerous invaluable nonlinear applications in sensor and communication fields [1–4]. The arrangement of air holes in the cladding region has gained more importance due to optical properties of PCF such as high nonlinearity, high birefringence, large mode-field area, high numerical aperture, ultra-flattened dispersion, adjustable zero dispersion, etc. [5–7]. Besides changing the geometry of the PCF, an alternative method to control its transmission and polarization properties is by filling the air holes, either completely or selectively, by various liquids such as CS_2, nitrobenzene, chloroform, water, ethanol, polymers and liquid crystals [8–11]. Recently, liquid core PCFs (LCPCFs) consisting of liquids in the core with numerous periodically spaced air holes in the cladding region have attracted a great deal of attention. This filling of liquids in PCF offers enormous increase in the nonlinearity value of

the fibre with adjustable dispersion and endlessly single mode operation. Because of their unique characteristics, various optical devices based on LCPCFs, such as zero dispersion fibres and mode coupling-based LCPCF devices have been investigated [6,7,9,10]. The increased interest in studying the properties of PCF is due to their potential soliton-related applications in various nonlinear domains [4–7]. The propagation of soliton in PCFs has been widely studied over the last decade or so. Soliton propagation in PCF having different structures is an attractive area of research and has hence led to great deal of scientific interest in both experiments and numerical simulation [12,13]. The crucial advantages of soliton using PCF over conventional fibre are well employed in many applications such as supercontinuum generation (SCG), pulse compression, optical switching, fibre laser, parametric amplifier, modulational instability (MI) etc. [3,6,14–16]. Even though several exciting research works have been carried out in PCF for various applications, generating broadband sources using SCG techniques finds many applications in the modern technological world [4,5]. The supercontinuum (SC) process is the intense ultra-fast broadband high coherent pulses spanning over few octaves, that has emerged as the technology of choice for future generation of broadband sources [4,5]. With the rapid advancement in PCF technology, SCG gains momentum and evolves as one of the most elegant and dramatic effect in optics with a wide range of potential applications in various fields such as frequency metrology, biomedical sensors, optical coherence tomography, wavelength division multiplexing, etc. [3–5].

SCG in a PCF was discovered by Ranka *et al* [17] as a means to generate a broad spectrum with two octave width at unprecedentedly low input pulse energies. Since then it has attracted extensive attention for both its fundamental and application aspects which were mainly motivated by its nonlinear applications in many research fields. Already lots of work were done on SCG in PCF in all pump regimes ranging from continuous wave, nanosecond, picosecond to femtosecond over the last decade [4,5]. For instance, in the femtosecond regime, when injecting 350 fs pulses using Yb^{3+}-doped fibre laser operating around 1060 nm, Price *et al* observed SCG over 400–1700 nm in PCF has a length of 7 m [18]. In parallel with these impressive results using femtosecond sources, there has been extensive interest in generating broadband SC by low-power picosecond and even nanosecond pulses. Thus, Nikolov *et al* generated a broad SC in a PCF using picosecond pulses and showed that the efficiency is significantly improved by proper dispersion design profile ensures that the Stokes and anti-Stokes bands generated by four-wave mixing directly from the pump to broaden, resulting in 800-nm-wide SC sources [19]. By using Yb^{3+}-doped fibre amplifier in a master oscillator power fibre amplifier at 1065 nm, Avodkhin *et al* generated SC of 1065–1375 nm wavelength range with high-power CW fibre sources using 100 m long PCF [20]. In addition to pulse duration, the effects of the input pulse parameters, such as pulse energy, peak power and central wavelength, on the SCG in PCF are subjects of high interest and have been thoroughly investigated in recent years [3–5].

SCG is typically achieved by two mechanisms, namely, soliton fission and MI [21,22]. The soliton fission leads to the generation of ultra-broadband spectrum, wherein pulse breaking arises mainly due to higher-order effects of soliton-related dynamics such as higher-order linear dispersion terms and nonlinear Raman scattering. The latter is the MI-induced SCG (MI-SCG), one of the fascinating manifestations of MI, which can achieve ultra-broadband spectrum [22,23]. The four-wave mixing (FWM) mechanism is actually

responsible for controlled MI process that allows manipulation and enhancement of the SCG process. Early investigations of MI-SCG were realized through conventional fibre in the region of low dispersion regime to enhance the broadband spectrum; later the idea has been effectively adopted to achieve the same in PCF. The fastest of such nonlinearities, the Kerr electronic nonlinearity, is responsible for the usual self-phase modulation, formation of the solitons in the anomalous regime, and is the basic mechanism for spectral broadening in many situations [4]. The second type of nonlinearity, the Raman nonlinearity, arises due to the excitation of the vibrational and rotational levels of the molecule and is responsible e.g. for the generation of Stokes and anti-Stokes bands and for the soliton self-frequency shift. Indeed, the broadening of the spectrum due to the Kerr nonlinearity is well known and has been thoroughly described. The same can be, to a certain extent, said about the Raman contribution to the nonlinearity. But, the nonlinearity of liquids (e.g. CS_2) often shows a complex temporal behaviour represented by the superposition of a fast electronic contribution and a delayed rotational and intermolecular contribution with a picosecond response time [21,22]. Because of the complex temporal behaviour of LCPCF, there are possibilities of new interesting properties of SCG. In particular, a third distinct type of non-linearity – reorientational nonlinearity and saturable nonlinearity – comes into play [21,22]. Thus, the main objective of this paper is to investigate the dynamical behaviour of SCG in LCPCF, filled with CS_2 liquid in the core. In particular, it is planned to study novel phys-ical phenomena related to the temporal and spectral changes of pulse propagating through specific PCFs such as LCPCF by the influence of saturable nonlinearity and reorientational nonlinearity.

2. Reorientational nonlinearity

The background mechanism of slow nonlinear response due to reorientational nonlinearity is the reorientation of the liquid molecules with a significant dipole moment in the electric field, which happens on typically 0.1 to 1 ps scale [21]. Therefore, this nonlinearity can be described as slow or retarded, since the modification of the refractive index depends on the field not only at the intensity at the given moment but also on the past. Such a slow nonlin-ear response plays an important role in the highly nonlinear materials such as nitrobenzene, chlorobenzene, chloroform and methylene chloride [24,25]. Note that this nonlinearity is different from Raman effect in terms of both the background mechanism and the mathe-matical description: the response function of the retarded nonlinearity is non-oscillating contrary to the response function of the Raman effect. For certain liquids, the retarded (reorientational) contribution to the nonlinearity can constitute as much as 90% of the total nonlinearity. This retarded nonlinearity can influence the soliton dynamics and therefore it plays an important role in the generation of SC. Besides that, other nonlinearity types, such as plasma-induced phase modulation, two-photon absorption, or thermal effects can lead to change in the properties of the material, but they can be neglected in this study for the considered intensities, material and time-scales. Raman effect can also be neglected in CS_2. Since the nonlinearity of CS_2-filled LCPCF is 100 times larger than that of silica core PCF [21,22], the nonlinearity induced by the reorientational contribution in the subpi-cosecond regime plays a notable role in the dynamics. Sato *et al* [26,27] had investigated the propagation dynamics and pulse compression in a fibre with CS_2 core. However, the

basic aspects of the influence of slow nonlinearity on the soliton dynamics and the SCG have not been systematically studied. The slow nonlinear response induces pulse break-ing in the presence of higher-order soliton dynamics which can subsequently expedite the soliton fission in CS_2-filled PCF. The retarded nonlinear response of the Kerr nonlinearity in liquids can modify the SCG mechanism and the coherence properties of the white light, which makes the study of SCG in LCPCF interesting from the fundamental point of view.

3. Theoretical model with reorientational nonlinearity

To study the influence of slow nonlinearity on the soliton propagation and stability as well as on the SCG in the case of the LCPCF, we consider a fibre with a cross-section consisting of a triangular lattice of circular air holes in fused silica, with 1.5 μm pitch and 1.3 μm hole diameter. One of the holes is filled with the CS_2 liquid, forming the core of the fibre. The schematic diagram of the liquid core PCF is shown in figure 1. In many realistic situations, as detailed in refs [26,27], the nonlinear response of the material to the ultra-short pulse field includes not only electronic contribution, but also reorientational contribution. Hence the total nonlinearity can be expressed as the sum of fast Kerr nonlinearity induced by elec-tronic contribution and slow nonlinearity induced by reorientational contribution, which is typically described by the response function with exponential decay in time. Reorienta-tional nonlinearity cannot be described as simply another form of Kerr nonlinearity. Indeed, the term which describes it in the equation is a completely different one. The dispersion to the third order, fast nonlinearity (Kerr-type) and reorientational nonlinearity are included in the model. In this case, to understand the dynamics of ultra-short pulse propagation in the presence of slow nonlinear response in LCPCF, we have used the modified nonlinear Schrödinger equation of the following form [28]:

$$\frac{\partial U}{\partial z} + \sum_{n=2}^{3} \beta_n \frac{i^{n-1}}{n!} \frac{\partial^n U}{\partial t^n} = i\gamma |U|^2 U + i\gamma_2 \mu U \int_0^\infty \exp(-\tau\mu)|U(t-\tau)|^2 \mathrm{d}\tau,$$

(1)
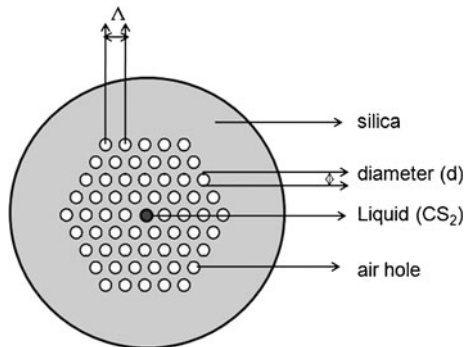
Figure 1. Schematic diagram of the liquid-core PCF with air hole diameter d and pitch Λ. The core is filled with CS_2 and has a diameter equal to the size of the air hole.

where U is the slowly varying envelope of the wave, z is the longitudinal coordinate and t is the time in the moving reference frame. The parameters β_n are the $n(=2,3)$th order dispersion coefficient, while the parameters γ and γ_2 describe the fast and reorientational nonlinearity and μ is the decay rate of the slow nonlinear polarization. To investigate the pulse propagation in PCF, we have numerically solved eq. (1) using split-step Fourier method (SSFM). The fibre parameters are evaluated using the fully vectorial effective index method (FVEIM) [29] which is a widely used numerical technique that provides a propagation constant of the guided modes in PCF, with the wavelength dependence of the refractive index of CS_2 included in the dispersion calculation. The wavelength dependence of the refractive index of CS_2 is given by [8]

$$n_{CS_2}(\lambda) = 1.580826 + 1.52389 \times 10^{-2} \times \lambda^{-2} + 4.8578 \times 10^{-4} \times \lambda^{-4}$$
$$-8.2863 \times 10^{-5} \times \lambda^{-6} + 1.4619 \times 10^{-5} \times \lambda^{-8}, \tag{2}$$

where λ is the wavelength in μm. The Kerr nonlinear coefficient γ is calculated using the formula $\gamma = n_2\omega_0/cA_{\text{eff}}$, where c is the velocity of light. Numerically, the effective area, A_{eff}, can be calculated as in ref. [26].

The effect of reorientational nonlinearity will be small for short pulses (below 50 fs), since the response does not have sufficient time to accumulate. On the other hand, for long pulses above several picoseconds duration, the effect of the reorientational nonlinearity will be indistinguishable from that of Kerr nonlinearity, at least at the initial stage of propagation. Therefore we have chosen 200-fs sech-shaped input pulse with central wavelength at 1200 nm. The fibre parameters are $\beta_2 = -0.109$ ps^2/m and $\beta_3 = 2.1 \times 10^{-4}$ ps^2/m, as calculated by our dispersion model, and the CS_2-filled core is characterized by $\gamma = 34.61$ W^{-1} m^{-1}, $\gamma_2 = 6\gamma$ and $\mu = 10$ ps^{-1} for LCPCF. We have neglected self-steepening since its effect is negligible to the perturbing effect of the third-order dispersion and retarded nonlinearity. Higher-order effects do not play a significant role, since the shape of the function β_3 is quite linear in the considered spectral range for our pulse parameters, and the corresponding higher-order dispersion coefficients are small.

4. SCG with reorientational nonlinearity

Inclusion of both fast and slow nonlinearities, as illustrated by figures 2 and 3, significantly changes the evolution of the single soliton. The retarded nonlinearity introduces the time-dependent phase shift which, contrary to the Kerr-type nonlinearity, has a nonzero derivative at the pulse peak. This leads to the shift of the pulse spectrum towards longer wavelengths, as visible in figure 2. Nevertheless, the soliton remains stable as a whole, despite the rapid change of its central frequency and amplitude. The reduction of amplitude, as shown in figure 2, occurs because the soliton sheds parts of its energy during the non-adiabatic frequency-shifting process and leaves behind a trace of relic radiation clearly seen in figure 2. This radiation should be distinguished from the non-solitonic radiation emitted by a soliton at the phase-matched position in the presence of third-order dispersion contribution; rather, it can be compared to the relic radiation emitted at the first stage of propagation in the case of unperturbed NLS equation, when the soliton number of the input pulse is a non-integer. Thus, we can conclude that the presence of the reorientational nonlinearity significantly changes the soliton dynamics, leading to a red-shift of the soliton
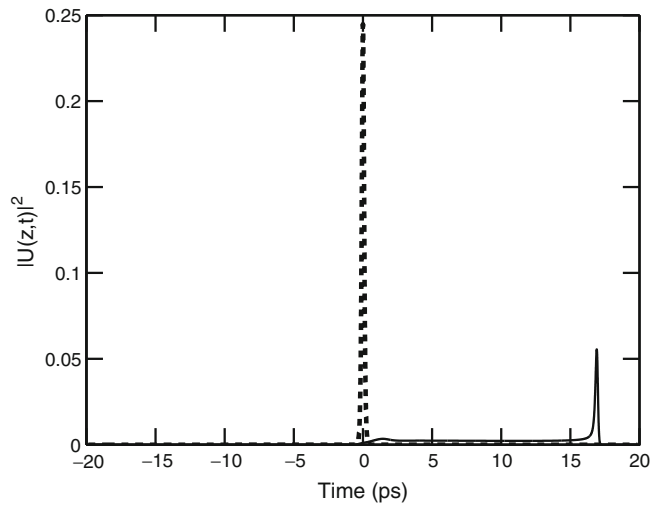
Figure 2. Fundamental soliton propagation of CS$_2$-filled LCPCF including slow nonlinearity (solid line). The solid line represents pulse evolution with slow nonlinearity where the decay constant $\mu = 10\,\mathrm{ps}^{-1}$ and slow nonlinearity $\gamma_2 = 6\gamma_0$. The dashed line represents soliton propagation in the absence of slow nonlinearity.

spectrum for the considered parameters, as well as to the emission of a dispersive wave seen as a pedestal in the temporal shape. Such a change of the dynamics cannot be described by perturbative treatment due to strong influence of the slow nonlinearity. However, the stability of the soliton is not jeopardized by the slow nonlinearity.
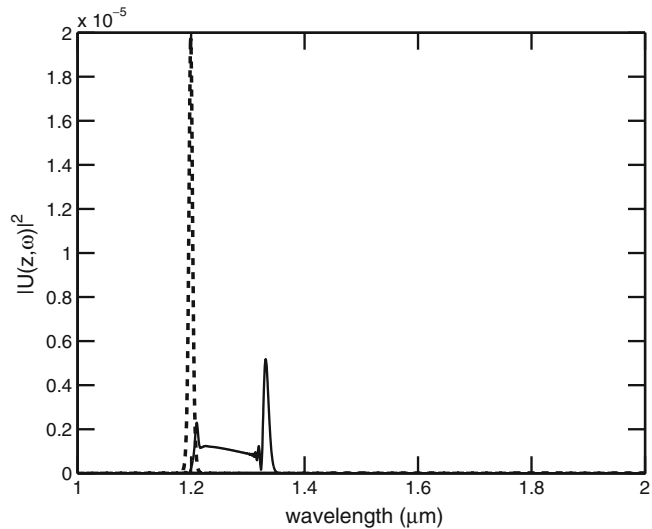

Figure 3. The stimulated spectral broadening of the 200 fs FWHM pulse in LCPCF without slow nonlinearity (dashed line) and with slow nonlinearity (solid line).
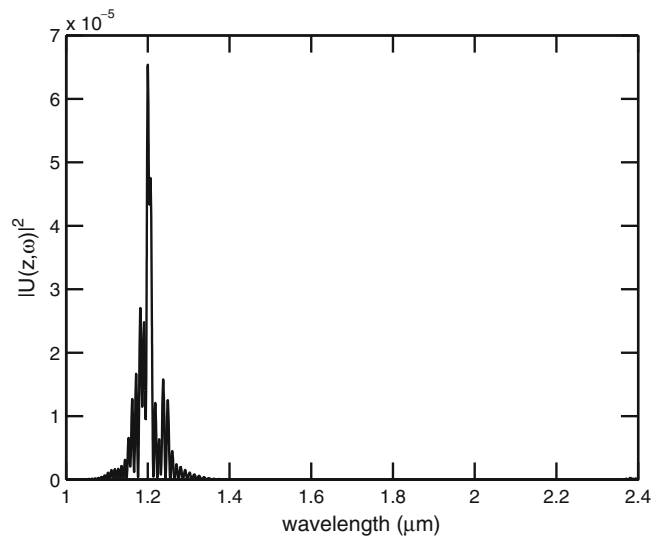
Figure 4. The evolution of seventh-order soliton spectral broadening through LCPCF in the absence of slow nonlinearity.

Let us now shift our attention to the input pulse with large soliton number. In figures 4 and 5, the spectra are shown for the input pulse with the soliton number of 7. It can be seen that the input pulse splits into several solitons, which manifest themselves as stable peaks in the temporal shape. Hence, we conclude that the solitons remain stable even if they are subjected to a combined disturbing action of slow nonlinearity and the presence
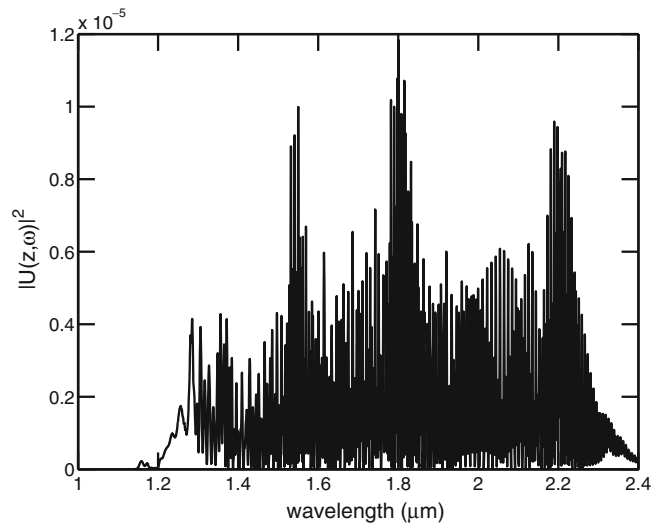
Figure 5. The evolution of seventh-order soliton spectral broadening through LCPCF in the presence of slow nonlinearity.

of other solitons. For the shortest sub-100-fs solitons, after fission, the dynamics is in fact dominated by the fast component.

Comparison of the spectral broadening in the presence and absence of the slow nonlinearity, which is given in figure 5, shows that the slow nonlinearity has a significant influence on the spectral broadening. For our parameters the spectrum of higher-order soliton, which is observed in the absence of slow nonlinearity, is not broad enough to seed the generation of the non-solitonic radiation. Therefore, the spectrum remains quite narrow, below one octave. In contrast, generation of a distinct peak of non-solitonic radiation by the soliton frequency shift and one-octave-broad spectrum is predicted when the slow nonlinearity is included.

As discussed in the previous section, the nonlinear response of CS_2 to the ultrashort pulse does not solely depend on the Kerr nonlinearity. But for the more realistic cases it includes the additional nonlinear effects like Raman response, reorientation contribution etc., in LCPCFs. Since the contribution of reorientational nonlinearity in SCG through CS_2-filled LCPCF have already been studied in the previous section, our investigation aimed at yet another type of nonlinear response, the so-called saturable nonlinearity. Hence the total nonlinearity can be expressed as the cumulative effect of both Kerr nonlinearity and the saturable nonlinearity. Thus, to analyse the dynamics of the ultra-short pulse propagation in LCPCFs in the presence of saturbale nonlinear response, the NLS equation needs to be modified.

5. Saturable nonlinear response

The detailed physical aspects of SCG can be interpreted by means of two mechanisms, namely, soliton fission and MI, as we already discussed. For ultra-short pulses typically in the femtosecond regime, higher-order dispersion and higher-order nonlinear effects such as third-order dispersion, fourth-order dispersion, Raman effect, self-steepening are measured as they play an increasingly important role in the spectral broadening process [4,5]. The Kerr nonlinearity is considered as the decisive agent in most of the common nonlinear phenomena such as self-phase modulation, the significant contender of many of the spectral broadening process observed in various domains. It is noteworthy that Kerr nonlinearity can only predict the nonlinear response of the medium for low input power. But in reality, for higher input power, higher-order nonlinear susceptibilities will inevitably come into play and eventually will saturate the nonlinear response of the medium [30]. Thus, at higher peak power, Kerr nonlinearity is not solely going to predict the associated nonlinear effects, but requires higher-order saturation effect to give a clear picture about the evolution of the SC spectrum. For instance, Kong *et al* [31] had investigated the quintic nonlinearity of the liquid CS_2, and it is apparent from their prediction that the quintic nonlinearity plays a vital role in the femtosecond regime. Since this quintic nonlinearity tends to saturate, one can expect a rich variety of information about the impact of saturation in the SCG mechanism and the subsequent influence on the coherence of the spectrum using LCPCF. The scenario that has not been addressed yet to our knowledge and thus seed the motivation is that 'what would happen to SCG if the light propagates in LCPCF with saturable nonlinear response?' Since most of the above investigations have used soliton fission for inducing SCG, we pursue another possibility of SCG using MI.

6. Theoretical model

To understand the mechanisms leading to the SCG, wave propagation in a single-mode fibre with higher-order dispersion and saturable nonlinearity (SNL) may be described by the following modified nonlinear Schrödinger equation [30]:

$$\frac{\partial U}{\partial z} + \sum_{n=2}^{4} \beta_n \frac{i^{n-1}}{n!} \frac{\partial^n U}{\partial t^n} - \frac{i\gamma |U|^2}{1 + \Gamma |U|^2} U = 0, \tag{3}$$

where $\Gamma = 1/P_s$ is the saturation parameter and P_s is the saturation power. In order to study the influence of SNL on the MI-SCG for LCPCF, we consider a fibre with a cross-section consisting of a triangular lattice of circular air holes in fused silica, with 1.8 μm and 1.44 μm as the pitch and hole diameter values respectively. To investigate the pulse propagation in PCF, we have numerically solved eq. (3) using SSFM with the initial envelope of the soliton at $z = 0$ given by $U(0, t) = \sqrt{P_0} \operatorname{sech}(t)$. Numerical simulations are carried out for the input pulse at the central wavelength $\lambda_0 = 1.06$ μm and a pulse width of 30 fs. The fibre parameters are $\beta_2 = -0.00041$ ps^2/m, $\beta_3 = 0.00078$ ps^3/m and $\beta_4 = 1.6 \times 10^{-7}$ ps^4/m and the nonlinearity value is $\gamma = 13.75$ W^{-1} m^{-1} for LCPCF.

7. MI-induced SCG in LCPCF

Before investigating MI-SCG in LCPCF, it is customary to switch off the effect of SNL for the better understanding of the MI spectrum. For the MI-SCG analysis, we have considered the amplitude perturbed soliton pulse with a peak power $P_0 = 400$ W. Figure 6
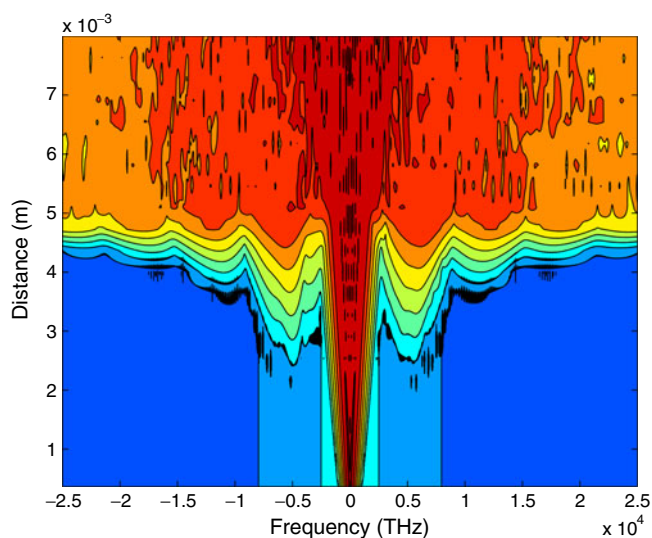
Figure 6. The SCG through MI of 30 fs pulse width in CS$_2$-filled LCPCF at 1.04 μm. The fibre parameters are $\beta_2 = -0.00041$ ps^2/m, $\beta_3 = 0.00078$ ps^3/m and $\beta_4 = 1.6 \times 10^{-7}$ ps^4/m and the nonlinearity $\gamma_0 = 13.75$ W^{-1} m^{-1}. The propagation length $L = 0.8$ cm.

depicts the MI-SCG spectrum for a propagation distance of $L = 0.8$ cm. It is observed that the pulse gets modulated due to noise perturbation which is signified by the emergence of the spectral side bands at the initial stage of propagation due to MI process, followed by further spectral broadening and the appearance of soliton structure on the long wavelength edge of the spectrum after 0.5 cm. This implies that, from the beginning, MI acts directly on the high-order soliton which leads to the generation of Stokes and anti-Stokes components. Because of perturbation such as higher-order dispersion and/or noise, the dynamics departs from the recurrent behaviour and results in pulse breaking. The fascinating point to observe from figure 6 is that the Stokes components emerge at shorter distance of pulse propagation with low power, overwhelming of the fact that nonlinear and dispersion values of CS$_2$-filled LCPCF are very large in comparison to the ordinary solid-core PCF. It is also evident from figure 6 that the pulse does not experience a notable asymmetric spectral broadening, which reflects the negligible role of higher-order effects in the chosen parameter region which is in agreement with Demircan and Bandelow [23]. The evolution of such primary spectral side bands at the initial stage of propagation will be accompanied by the emergence of secondary side bands after a distance $z = 0.25$ cm. Then the subsequent spectral broadening accomplished through FWM seeded by phase matching explosively excites new frequencies and thus broadens the spectrum. Thus, one can achieve a broad spectrum, typically SC, at a relatively short distance of propagation using low input power in LCPCF when compared to silica-core PCF. Simultaneously, we have also analysed the evolution of MI dynamics in time domain from figure 7. It is obvious from figure 7 that, as there is no phase matching between linear and nonlinear effects at the beginning, pulse breaking is limited at the initial stage. But for a relatively higher distance, typically $z = 0.5$ cm and above, the required phase matching can be satisfactorily achieved and thus
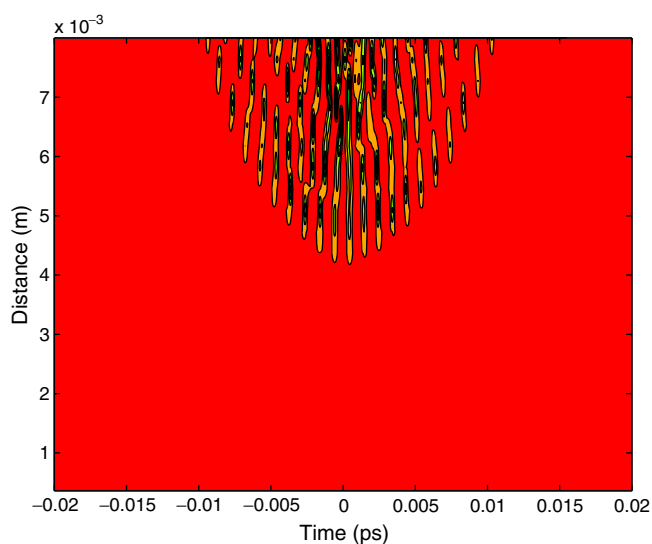
Figure 7. The pulse propagation through CS$_2$-filled LCPCF. The fibre parameters are $\beta_2 = -0.00041$ ps^2/m, $\beta_3 = 0.00078$ ps^3/m and $\beta_4 = 1.6 \times 10^{-7}$ ps^4/m and the nonlinearity $\gamma_0 = 13.75$ W^{-1} m^{-1}. The propagation length $L = 0.8$ cm.

the pulse breaking starts due to the formation of ripples in the temporal intensity profile. These ripples get spread out with further propagation thus covering the whole spectrum, resulting in the fine structure of SC spectrum.

8. MI-SCG in the presence of saturable nonlinearity

Now in this context, we shift our attention towards the prime objective of the work, the effect of SNL in the MI spectrum. Considering the PCF structure as in the preceding section, we begin to explore the effect of SNL in the SC spectrum. The process of MI leading to SC can be understood by the weak perturbation of the steady-state solution. The steady-state solution of eq. (3) can be written as [30]

$$U_s = \sqrt{P_0}\exp[i\phi(z)], \tag{4}$$

where P_0 is the input pump power and ϕ is the nonlinear phase shift which can be defined as

$$\phi(z) = \frac{\gamma P_0 z}{1 + \Gamma P_0}. \tag{5}$$

The linear stability of the steady state can be examined by introducing a perturbed field of the following form:

$$U = (\sqrt{P_0} + q(z, t))\exp[i\phi(z)], \tag{6}$$

where $|q|^2 \ll P_0$. For the perturbation, we assume the following ansatz with frequency detuning from the pump Ω:

$$q(z, t) = u(z)\exp(-i\Omega t) + v(z)\exp(i\Omega t), \tag{7}$$

where $u(z)$ and $v(z)$ are the complex perturbation amplitudes corresponding to the anti-Stokes and Stokes side bands, respectively. By substituting eqs (6) and (7) in eq. (3), and collecting the linear terms in $u(z)$ and $v(z)$, we obtain the following equation for the perturbed field:

$$\frac{dY}{dz} = iMY = \begin{pmatrix} D(\Omega) + \tilde{\gamma} & \tilde{\gamma}P_0 \\ -\tilde{\gamma}P_0 & -D(\Omega) - \tilde{\gamma} \end{pmatrix}, \tag{8}$$

where

$$Y = \begin{pmatrix} u(z) \\ v(z) \end{pmatrix}, \tag{9}$$

$$D(\Omega) \equiv \beta_2\frac{\Omega^2}{2} - \beta_3\frac{\Omega^3}{6} + \beta_4\frac{\Omega^4}{24}, \tag{10}$$

$$\tilde{D}(\Omega) \equiv \beta_2\frac{\Omega^2}{2} + \beta_3\frac{\Omega^3}{6} + \beta_4\frac{\Omega^4}{24}, \tag{11}$$

$$\tilde{\gamma} \equiv \gamma/(1 + \Gamma P_0)^2, \tag{12}$$

$$Q \equiv 1 + \Gamma P_0. \tag{13}$$

The eigenvalues of the stability matrix M determine the wavenumber K of the perturbation. MI occurs when K possesses a non-zero imaginary part. The eigenvalues of M are given by the following dispersion relation:

$$K^2 + [\tilde{D}(\Omega) - D(\Omega)]K - \frac{\gamma P_0}{Q^2}[\tilde{D}(\Omega) + D(\Omega)] - \tilde{D}(\Omega)D(\Omega) = 0, \tag{14}$$

which can be rewritten after simple algebraic manipulations as

$$K = -\beta_3 \frac{\Omega^3}{6} \pm \sqrt{\left(\tilde{\gamma}P_0 + \beta_2 \frac{\Omega^2}{2} + \beta_4 \frac{\Omega^4}{24}\right)^2 - \tilde{\gamma}^2 P_0^2}. \tag{15}$$

The gain spectrum is given by

$$G(\Omega) = 2\,\mathrm{Im}(K) = 4\sqrt{\tilde{\gamma}^2 P_0^2 - \left(\tilde{\gamma}P_0 + \beta_2 \frac{\Omega^2}{2} + \beta_4 \frac{\Omega^4}{24}\right)^2}. \tag{16}$$

It is quite interesting to observe that, as in the case of unsaturated nonlinearity, the third-order dispersion is insignificant and does not play any role in the gain of the spectrum. The equation offers a rich variety of information which can be efficiently exploited in many ways.

For large negative β_2 values, the higher-order dispersion effects are relatively negligible. In this dispersion domain the SNL leads to critical modulational frequency as

$$\Omega_c = \left[\frac{4\gamma P_0}{|\beta_2|(1 + \Gamma P_0)^2}\right]^{1/2}.$$

In the typical operating condition of unsaturated PCF, the required phase matching to acquire MI is achieved through the compensation of second-order dispersion with Kerr nonlinearity. Quite interestingly, in LCPCF, the incorporation of SNL of the medium encounters additional phase shift to achieve the phase matching. Such a condition leads to behaviours that qualitatively differ depending on the magnitude of dispersion and saturation power, thus emphasizing the sensitivity of MI towards the saturation power and dispersion on the MI spectrum. Since the MI bandwidth increases as Γ decreases, the effect of MI can be very strong for high saturation power. In the vicinity of near zero-dispersion regime, the fourth-order dispersion enters inevitably into play. Hence in the fourth-order dispersion dominant system, the critical modulational frequency is given by

$$\Omega_{\mathrm{opt}} = \left[\frac{48\gamma P_0}{|\beta_4|(1 + \Gamma P_0)^2}\right]^{1/2}.$$

For $\Gamma = 0$, it is noteworthy that the MI gain and critical frequencies coincide exactly with the case of unsaturated nonlinearity as discussed in ref. [23]. Since the focus of the paper

is to investigate the influence of SNL, we have considered the PCF parameter with large β_2 value. Although the higher-order dispersion coefficients are momentous in PCF, the role of sixth-order dispersion is literally insignificant for MI for our further investigations in the given PCF structure. Hence we limit ourselves upto fourth-order dispersion. In order to investigate the dynamical behaviour of the MI process under SNL, we consider the same PCF parameters as in the preceding section.

From our numerical simulation, we have obtained the results as depicted in figures 8 and 9 which show the effect of SNL for fixed saturation power $P_s = 2000$ W. By including SNL, the evolution of the MI significantly changes as illustrated in figure 8. As per the critical frequency condition, due to the saturation effects, the phase matching can only be achieved at longer distance in comparison to that of the unsaturated nonlinearity. Thus, the SNL certainly suppresses the MI process as illustrated in figure 8. Hence, the spectral broadening can only be obtained at longer distance when compared to unsaturated fibre. The corresponding dynamics of pulse breaking in time domain is portrayed in figure 9. Since the phase matching between linear and nonlinear effects is influenced by the SNL, the pulse breaking can only be achieved at comparatively longer distance than the unsaturated LCPCF. For a better insight into the picture of MI-SCG, we have investigated the evolution of MI for various saturation powers as in figure 10. In the operating conditions of saturated nonlinearity, the optical modulational frequency not only varies with the input power of pulse but also with saturation power as illustrated in figure 10. It is observed that the evolution of MI in LCPCF is certainly suppressed by the decreasing saturation powers, which means that while increasing the SNL the MI-SCG gets suppressed. Figure 11 depicts spectral evolution of MI-SCG in the presence of SNL with different saturation powers.
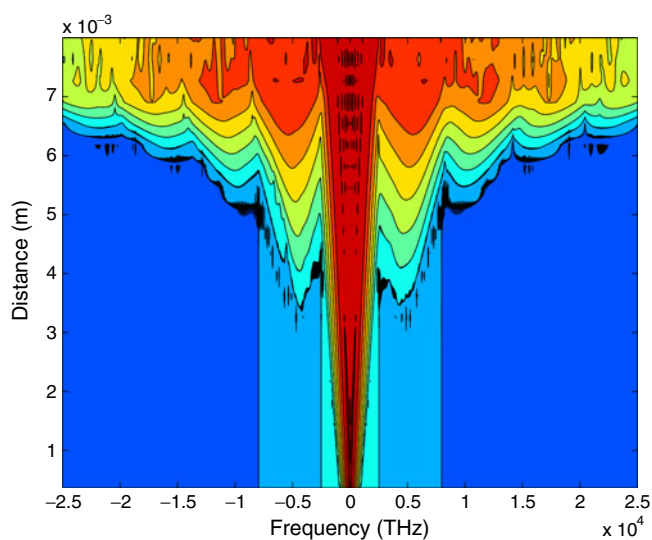

Figure 8. The MI-SCG with saturable nonlinearity for 30 fs of pulse width in CS$_2$-filled LCPCF at 1.04 μm. $\beta_2 = -0.00041$ ps^2/m, $\beta_3 = 0.00078$ ps^3/m and $\beta_4 = 1.6 \times 10^{-7}$ ps^4/m and the nonlinearity $\gamma_0 = 13.75$ W^{-1} m^{-1} with saturable power $P_s = 2000$ W. The propagation length $L = 0.8$ cm.
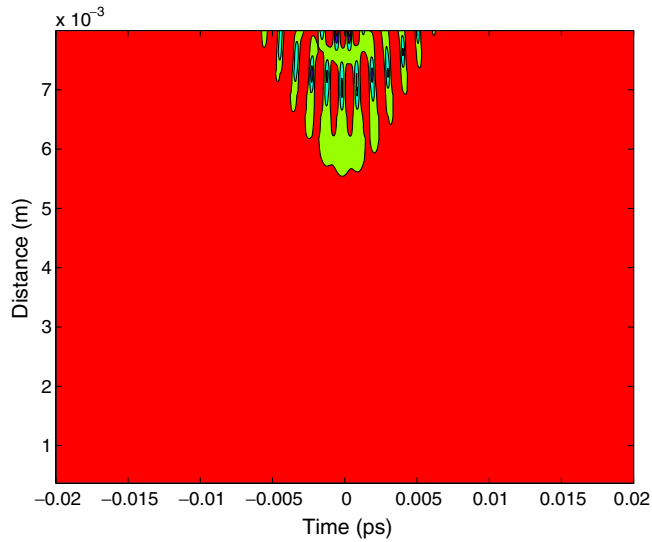
Figure 9. The pulse propagation through CS_2-filled LCPCF with saturable nonlinearity. The fibre parameters are $\beta_2 = -0.00041$ ps^2/m, $\beta_3 = 0.00078$ ps^3/m and $\beta_4 = 1.6 \times 10^{-7}$ ps^4/m and the nonlinearity $\gamma_0 = 13.75$ W^{-1} m^{-1} with saturable power $P_s = 2000$ W. The propagation length $L = 0.8$ cm.

It is obvious from figure 11 that the saturable LCPCF also shows flat spectrum, where the spectral density at the peak varies merely less than 10 dB over a bandwidth of 800–1500 nm. It is also observed that the spectral broadening quantitatively gets suppressed with decrease in the saturation power.
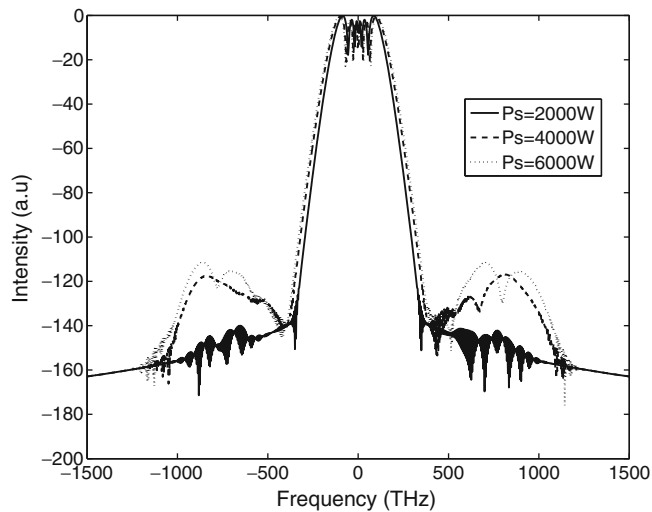
Figure 10. The evolution of MI phenomena for 30 fs pulse in LCPCF with different saturable powers.
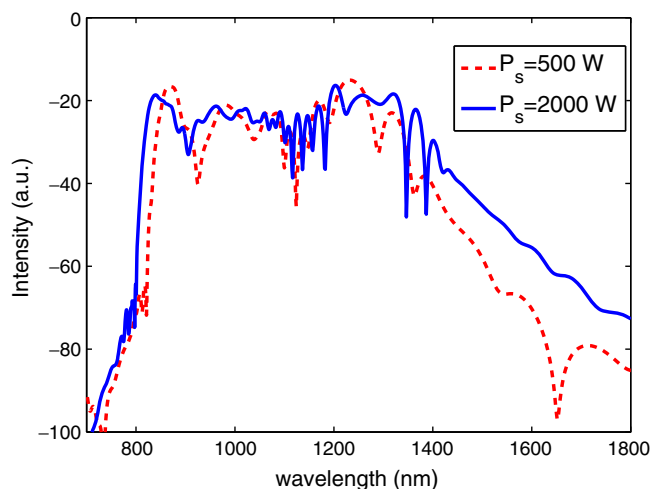
Figure 11. SCG using MI for different saturation powers.

9. Conclusion

We have theoretically investigated the nonlinear propagation of femtosecond pulses in LCPCF filled with CS_2. First, the effect of slow nonlinearity due to reorientational contribution of liquid molecules on broadband SCG in the femtosecond regime has been studied using appropriately modified nonlinear Schrödinger equation. We show that the response of the slow nonlinearity not only enhances broadening of the pulse and changes the dynamics of the generated solitons, but also increases coherence of the pulse. Finally, we theoretically investigate the SCG on the basis of MI in LCPCF with CS_2-filled central core to study the effect of saturable nonlinearity on SCG. We also compare the MI-induced spectral broadening with SCG obtained by soliton fission. The quality of the pulse broadening has been analysed by calculating the coherence of the SC pulse through numerical simulation. It is evident from the numerical simulation that the response of the saturable nonlinearity suppresses the broadening of the pulse. Also it has been observed that the MI-induced SCG in the presence of saturable nonlinearity degrades the coherence of the SCG pulse when compared to unsaturated medium.

Acknowledgements

References

[1] P St J Russell, *Science* **299**, 358 (2003)
[2] J M Dudley and J R Taylor, *Nat. Photon.* **3**, 85 (2009)
[3] A M Zheltikov, *Physics-Uspekhi*, **49(6)**, 605 (2006)

[4] J M Dudley and J R Taylor (eds) *Optical fibre supercontinuum generation,* 1st edn (Cambridge University Press, Cambridge, 2010)

[5] J M Dudley, G Genty and S Coen, *Rev. Mod. Phys.* **78**, 1135 (2006)

[6] R Vasantha Jayakantha Raja, K Senthilnathan, K Porsezian and K Nakkeeran, *IEEE-J. Quant. Elect.* **46**, 1795 (2010)

[7] R Vasantha Jayakantha Raja, K Porsezian, Shailendra K Varshney and S Sivabalan, *Opt. Commun.* **283**, 5000 (2010)

[8] R Zhang, J Teipel and H Giessen, *Opt. Express* **14**, 6800 (2006)

[9] M Vieweg, T Gissibl, S Pricking, B T Kuhlmey, D C Wu, B J Eggleton and H Giessen, *Opt. Express* **18**, 25232 (2010)

[10] S Yiou, P Delaye, A Rouvie, J Chinaud, R Frey and G Roosen, *Opt. Express* **13**, 4786 (2005)

[11] C J S de Matos, C M B Cordeiro, M E dos Santos, J S K Ong, A Bozolan and C H B Cruz, *Opt. Express* **15**, 11207 (2007)

[12] D V Skryabin and A V Gorbach, *Rev. Mod. Phys.* **82**, 1287 (2010)

[13] J M Dudley, G Genty, F Dias, B Kibler and N Akhmediev, *Opt. Express* **17**, 21497 (2009)

[14] F W Wise, A Chong and W H Renninger, *Laser Photon. Rev.* **2**, 58 (2008)

[15] M H Frosz, T Sørensen and O Bang, *J. Opt. Soc. Am.* **B23**, 1692 (2006)

[16] A K Sarma, *Jpn J. Appl. Phys.* **47**, 5493 (2008)

[17] J K Ranka, R S Windeler and A J Stentz, *Opt. Lett.* **25**, 25 (2000)

[18] J H V Price, K Furusawa, T M Monro, L Lefort and D J Richardson, *J. Opt. Soc. Am.* **B19**, 1286 (2002)

[19] N I Nikolov, T Sørensen, O Bang and A Bjarklev, *J. Opt. Soc. Am.* **B20**, 2329 (2003)

[20] A V Avdokhin, S V Popov and J R Taylor, *Opt. Lett.* **28**, 1353 (2003)

[21] R Vasantha Jayakantha Raja, A Husakou, J Hermann and K Porsezian, *J. Opt. Soc. Am.* **B27**, 1763 (2010)

[22] R Vasantha Jayakantha Raja, K Porsezian and K Nithyanandan, *Phys. Rev.* **A82**, 013825 (2010)

[23] A Demircan and U Bandelow, *Appl. Phys.* **B86**, 31 (2007)

[24] R W Hellwarth, *Prog. Quant. Electr.* **5**, 1 (1977)

[25] D McMorrow, W T Lotshaw and G A Kenney-wallace, *IEEE-J. Quant. Elect.* **24**, 443 (1988)

[26] Y Sato, R Morita and M Yamashita, *Jpn J. Appl. Phys.* **36**, 6768 (1997)

[27] Y Sato, R Morita and M Yamashita, *Jpn J. Appl. Phys.* **36**, 2109 (1997)

[28] G P Agrawal, *Nonlinear fibre optics* (Academic Press, 2001)

[29] R Vasantha Jayakantha Raja and K Porsezian, *J. Photon. Nanostruct. -Fundamentals and Applications* **5**, 171 (2007)

[30] P T Dinda and K Porsezian, *J. Opt. Soc. Am.* **B27**, 1143 (2010)

[31] D G Kong, Q Chang, H Ye,Ya Chen Gao, Y X Wang, X R Zhang, K Yang, W Zhi Wu and Y L Song, *J. Phys. B: At. Mol. Opt. Phys.* **42**, 065401 (2009)